

*Original Research*

# Geochemical Behaviours and Formation Mechanisms for Elevated Fluoride in the Drinking Groundwater in Sulin Coal-Mining District, Northern Anhui Province, China

Chunming Hao<sup>1,2,3</sup>, Wei Zhang<sup>1</sup>, Herong Gui<sup>2\*</sup>

<sup>1</sup>North China Institute of Science and Technology, Hebei, 065201, P.R. China

<sup>2</sup>National Engineering Research Center of Coal Mine Water Hazard Controlling (Suzhou University), Anhui, 234000, P.R. China

<sup>3</sup>State Key Laboratory of Groundwater Protection and Utilization by Coal Mining, Beijing, 100011, P.R. China

*Received: 1 June 2020*

*Accepted: 4 December 2020*

## Abstract

There has been substantial research on the sources and geochemical processes associated with fluoride (F<sup>-</sup>) in agricultural groundwater. However, the spatial distribution, geochemical behaviours, and enrichment mechanisms of fluoride in the groundwater from a coal-mining district used for drinking water supply have not been fully understood. In this study, 42 drinking water samples of the groundwater were collected in May 2019 and March 2020 from the Sulin coal-mining district, Anhui, China. Samples were analysed to investigate the distribution, geochemical behaviour, and formation mechanisms of fluoride. The F<sup>-</sup> concentrations in the groundwater samples ranged from 0.55 to 2.06 mg/L, with a mean value of 1.16 mg/L. The F<sup>-</sup> concentrations in 54.76% of the water samples exceeded China's national standards (1.00 mg/L). The results show that the F<sup>-</sup> in the water was enriched in an environment with high pH and HCO<sub>3</sub><sup>-</sup> content. The weathering of F<sup>-</sup> bearing minerals was the main source of F<sup>-</sup> in the drinking water supply. Evaporation, cation exchange, competitive effect, and anthropogenic activities were considered to have promoted elevated F<sup>-</sup> concentrations in the groundwater resource. This research will aid policy development for properly managing drinking water to eliminate health problems in coal-mining districts due to excessive fluoride intake.

**Keywords:** high fluoride, geochemical behaviour, fluoride enrichment mechanism, groundwater resource

## Introduction

Fluorine (F) is a nonmetal element that is rarely present in its elemental form in nature as a result of its high chemical activity. As such, fluorine mostly occurs in the form of chemical compounds that are widely distributed throughout surface water, groundwater, and oceans [1, 2]. Groundwater is the principal source of fluoride (F<sup>-</sup>) for human ingestion; it is controlled by low groundwater infiltration and flow rates, leading to prolonged water-rock interactions [2-4]. Excess F<sup>-</sup> intake can lead to dental and skeletal diseases; as such, the ingestion of fluoride through drinking water has gained widespread attention [3, 4]. As excess fluoride is a public health concern, World Health Organisation (WHO) limits maximum F<sup>-</sup> content in drinking water to 1.50 mg/L [4-7]. Water bodies with an F<sup>-</sup> content above this maximum are considered unsuitable drinking water sources. The occurrence of groundwater with high F<sup>-</sup> concentrations has been reported around the world; this is particularly problematic in China, India, Kenya, Iran, Pakistan, and Jordan [1-2, 4, 8-10]. The levels of F<sup>-</sup> exceed 18.50 mg/L in India [2], whilst in Pakistan, the F<sup>-</sup> concentration is up to 44.40 mg/L [9]. More than 41 million people in China have ingested high-fluoride groundwater. This groundwater is widely distributed throughout Inner Mongolia, Shanxi, Jilin, Anhui, and Gansu [11-4]. As such, the maximum permissible F<sup>-</sup> concentration in drinking water in China is 1.00 mg/L [11].

Fluorite (CaF<sub>2</sub>), fluorapatite [Ca<sub>5</sub>(PO<sub>4</sub>)<sub>3</sub>F], biotite [K(Mg,Fe)<sub>3</sub>(AlSi<sub>3</sub>O<sub>10</sub>)(OH,F)], phlogopite [KMg<sub>3</sub>(AlSi<sub>3</sub>O<sub>10</sub>)], and hornblende [CaNa(Mg, Fe, Al)(Si,Al)O<sub>22</sub>(OH, F)<sub>2</sub>] are common F-bearing minerals [13-17]. Higher levels of fluoride are generally associated with high pH [17-20] and Na-HCO<sub>3</sub> type waters [1, 6, 21], although the evaporation and ion exchange factors [4, 10, 22, 23] may also play an important role in promoting elevated F<sup>-</sup> concentrations in groundwater. In addition to natural processes, F<sup>-</sup> concentration in groundwater can also increase owing to anthropogenic activities such as intensive agricultural activities, poorly planned urbanisation, and industrial and mining activities [9, 24, 25].

In the northern Anhui Province of China, deep confined aquifers in the thick loose-bed seam are the primary sources of drinking water. Numerous studies have been conducted on geochemistry [26-28], water-rock interactions [29, 30], and heavy metal pollution [31] of these deep confined aquifers in the Sulin coal-mining district. These studies aimed to prevent the entry of deep confined water into the mining wells as this is a hazard in coal mining. Little attention has been directed at drinking water supply aquifers as the impact of coal mining on these resources is considered to be slight. Studies have found that the F<sup>-</sup> content in drinking water aquifers in this area has reached 3.10 mg/L [12]; this is typical of high-fluoride content drinking water. Based on a rough estimation, approximately

5.6 million people in the area have been drinking high-fluoride groundwater for a long time. Moreover, almost half of the population lives in rural areas without the proper protection measures; approximately 60% suffer from dental fluorosis, of which 10% show symptoms of skeletal fluorosis [14, 32]. Despite this, few studies have been conducted on the spatial distribution and geochemical behaviour of F<sup>-</sup> in drinking water aquifers in this area; the sources and formation mechanisms of high-fluoride content groundwater remain unclear.

This study addresses three key objectives: (1) to evaluate the abundance and spatial distribution of F<sup>-</sup> in groundwater that is used as a primary drinking water resource; (2) to evaluate differences in geochemical behaviours between high-fluoride and low-fluoride groundwaters; and (3) to understand the mechanism behind high-fluoride content groundwater in the study area.

## Material and Methods

### Regional Geology and Hydrogeology

Sulin coal-mining district has an area of approximately 100 km<sup>2</sup>. It is located in the alluvial plain of the Yellow and Huaihe rivers in the northern part of Anhui Province, China. Its geographical coordinates are 116°15'-117°12'E and 33°20'-33°42'N. The area experiences a sub-humid monsoon climate, where the mean annual precipitation and evaporation is 860 and 1060 mm, respectively. In addition, the annual mean temperature is approximately 14-15°C. The wind in the area is predominantly by the southeasterlies. The Huaihe River system is the main water system, including Tuo, Hui, Xie, and Guo rivers. These rivers flow from the northwest to the southeast before entering the sea. The mean annual flow of these rivers ranges from 3.52 to 72.10 m<sup>3</sup>/s.

Sulin coal-mining district is surrounded by the Ban Qiao Fault to the south, the Su Bei Fault to the north, and the Feng Wo Fault to the west (Fig. 1). As a concealed type colliery, coal deposits in the Sulin coal-mining district are covered by loose sediments. The thickness of the coal exceeds 1300 m, including three to 12 minable and locally minable coal seams. The area contained 19 coal mines with a total production capacity of 30.00 million t/y [33, 34]. After 69 years of mining, a large number of collapsed ponds and coal gangue piles have accumulated on the land surface [35]. Aside from the mining area, most of the land in this area is dedicated to agriculture where wheat and corn are the primary crops. The study area is lacking in surface water, and groundwater is the main source of water for domestic and industrial purposes [33].

Sulin coal-mining district is covered by a Quaternary loose layer that has a thickness of 100.50-771.70 m. The Cenozoic group in the study area

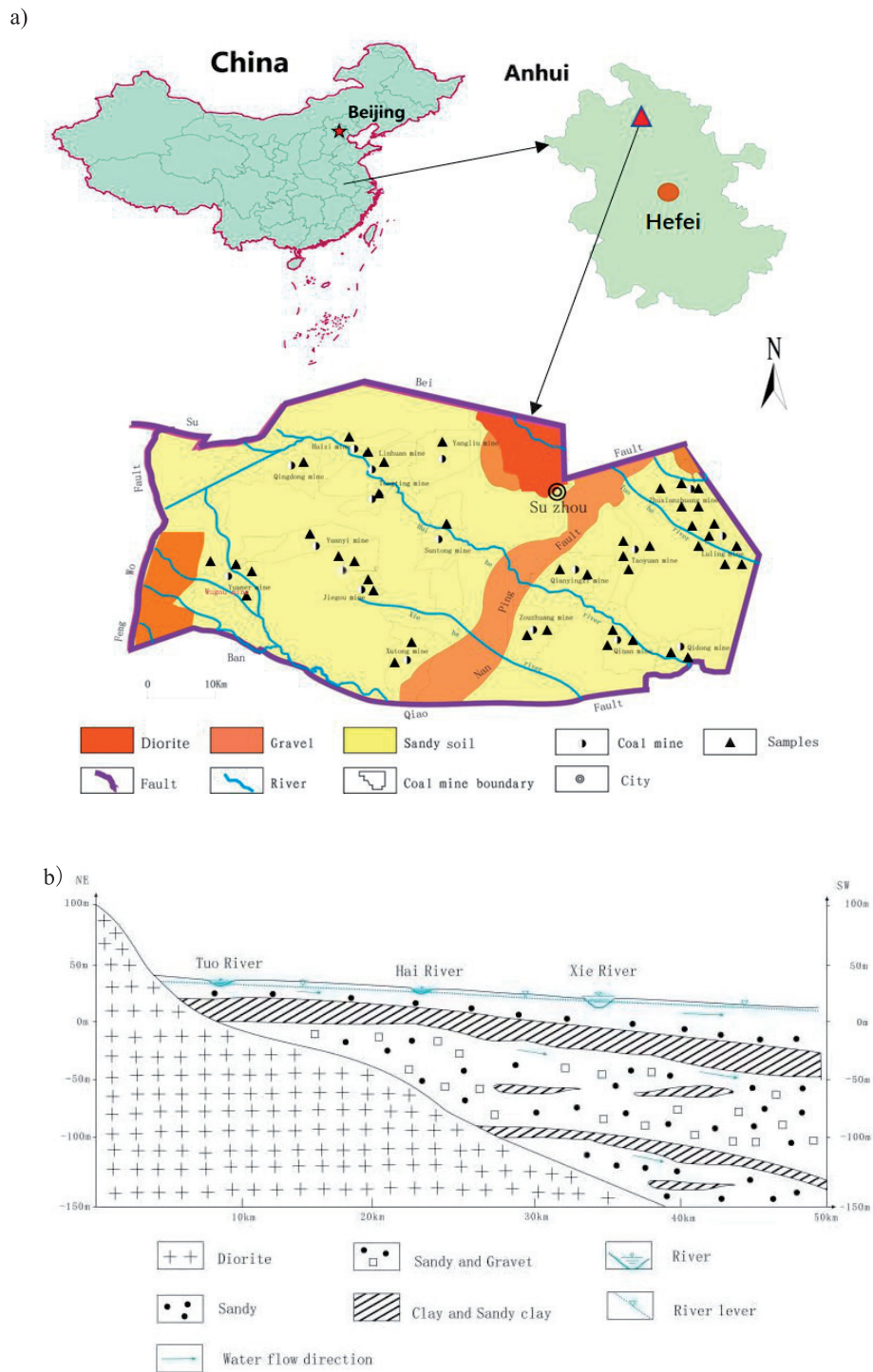


Fig. 1. a) Location of the study area and sampling sites. b) Schematic hydrogeological cross-section.

contains four aquifers; these are, from top to bottom, the first, second, third, and fourth aquifers. The second and third aquifers (80-130 m in depth, and a mean depth of 110 m) are widely used as the drinking water supply due to their abundant and high-quality groundwater [33]. The main components of the water-bearing medium are gravel and sand. As a confined aquifer, drinking water aquifers have poor hydraulic connections with lateral precipitation recharge, slow surface runoff, and excretion [33].

### Sample Collection and Analysis

Fig. 1a) shows that a total of 42 groundwater samples from the drinking water supply were collected in May 2019 and March 2020. Prior to sample collection, the groundwater at every sampling site was drained for 10 to 15 min to access fresh groundwater. Sampling plastic bottles were first washed with distilled water two to three times and then washed with sample water another two to three times. Collected water samples

were all filtered using filter membranes with a pore size of 0.45  $\mu\text{m}$  before being stored in the washed sampling plastic bottles. For each sampling site, three bottles (500 mL each) of the water samples were collected. To improve the analytical accuracy of the  $\text{F}^-$  concentration, 5 mL of  $\text{F}^-$  standard solution (1.00 mg/L) was added as the recovery indicator in each water sample. The pH and concentration of total dissolved solids (TDS) were measured in the field using a portable pH metre (OHAUS ST20) and a portable TDS metre (OHAUS ST20T-B), respectively.

Concentrations of anions ( $\text{Cl}^-$ ,  $\text{SO}_4^{2-}$ ,  $\text{NO}_3^-$ , and  $\text{F}^-$ ) and cations ( $\text{Ca}^{2+}$ ,  $\text{Mg}^{2+}$ ,  $\text{Na}^+$ , and  $\text{K}^+$ ) were determined by ion chromatography (Dionex Integrion IC, Thermo Fisher, USA). Prior to chemical analysis, instruments were calibrated against existing standards, and method detection limits were calculated by replacing with the proper citations. The concentrations of carbonates and bicarbonate anions were measured through acid-base titrations in the laboratory. Analytical grade reagents were used.

### Analytical Quality Control

Each water sample had three duplicates, and each analysis was carried out in triplicate to ensure that the standard deviation was below 10%. Nine data points were averaged into one final data point to obtain the mean and the standard deviation. This means the final 42 test data points for the groundwater samples reported in this study analysing TDS, pH,  $\text{Cl}^-$ ,  $\text{SO}_4^{2-}$ ,  $\text{NO}_3^-$ ,  $\text{HCO}_3^-$ ,  $\text{F}^-$ ,  $\text{Ca}^{2+}$ ,  $\text{Mg}^{2+}$ ,  $\text{Na}^+$ , and  $\text{K}^+$  are the mean values of 378 test results. The recovery rate of the recovery indicator was between 95% to 105%. The analytical precision of ion concentrations was confirmed by calculating the ionic balance errors; these errors were generally within  $\pm 5\%$ . Additionally, 20% of the samples were randomly selected for re-analysis. The errors between the first and second analysis results were below  $\pm 10.00\%$ .

## Results

### Geochemical Characterisation

The geochemical characterisation of the groundwater samples is presented in Table 1. The pH of the water samples ranged from 7.20 to 8.28, with a mean value of 7.89. This indicates that the water body presented a weakly alkaline environment and that the samples are within China's national standards – 6.50 to 8.50 – for drinking water [36].  $\text{Na}^+ + \text{K}^+$  were the dominant cations present and their cumulative content ranged from 20.32 to 311.24 mg/L, with a mean value of 141.23 mg/L.  $\text{Mg}^{2+}$  was the second most abundant cation ranging between 17.62 and 150.19 mg/L, with a mean value of 52.96 mg/L. The content of  $\text{Ca}^{2+}$  ranged from 15.16 to 76.01 mg/L, with a mean content of 39.80 mg/L; this is the lowest among the four cations.  $\text{Mg}^{2+}$  had a higher concentration than  $\text{Ca}^{2+}$ . This may be due to the evapotranspiration precipitation of  $\text{Ca}^{2+}$ . The anion concentrations in these water samples included (from highest to lowest) a  $\text{HCO}_3^-$  concentration between 300.61 and 853.02 mg/L (mean of 498.61 mg/L), a  $\text{SO}_4^{2-}$  concentration between 12.03 and 462.39 mg/L (mean of 151.23 mg/L), and a  $\text{Cl}^-$  concentration between 4.33 and 216.6 mg/L (mean of 72.30 mg/L). The  $\text{SO}_4^{2-}$  content in 19.05% of the samples exceeded China's national standards (250.0 mg/L) for drinking water. The TDS concentrations were between 319 and 1564 mg/L, with a mean of 958 mg/L. The TDS in 35.71% of the samples exceeded China's national standards (1000 mg/L) for drinking water.

The piper diagram illustrates distinguishable geochemical features in the drinking groundwater samples [37]. Fig. 2 shows that the geochemical facies of the drinking groundwater samples were Na-Mg- $\text{HCO}_3^-$  (46.62%), Na-Mg- $\text{HCO}_3^-$ - $\text{SO}_4^{2-}$  (38.10%), and Na- $\text{HCO}_3^-$  (9.520%).

The  $\text{F}^-$  concentrations in the groundwater samples ranged from 0.16 to 2.06 mg/L, with a mean of 1.11 mg/L. Among these samples, 54.76% had elevated  $\text{F}^-$  concentrations that exceeded China's national

Table 1. Geochemical data for the samples collected in the study.

Types		$\text{K}^+$	$\text{Na}^+$	$\text{Ca}^{2+}$	$\text{Mg}^{2+}$	$\text{SO}_4^{2-}$	$\text{Cl}^-$	$\text{F}^-$	$\text{HCO}_3^-$	$\text{NO}_3^-$	TDS	pH
		mg/L										
Max	Low-fluoride drinking groundwater (n = 19)	4.110	218.5	69.20	94.49	459.5	184.1	0.9800	488.9	5.790	1385	8.060
Min		0.230	20.32	35.53	17.62	12.03	4.33	0.1600	300.6	0.000	319.0	7.200
Mean		1.120	106.8	52.29	52.25	164.2	75.79	0.7100	421.8	0.670	838.0	7.710
SD		1.190	60.24	19.62	19.62	121.2	44.40	0.2400	104.9	1.670	308.6	0.310
Max	High-fluoride drinking groundwater (n = 23)	1.85	311.2	76.01	150.2	462.4	216.6	2.060	853.0	8.510	1564	8.280
Min		0.16	86.53	15.16	25.51	24.22	11.71	1.040	321.6	0.000	721.0	7.790
Mean		0.55	169.6	34.26	53.98	140.5	69.41	1.440	566.3	1.290	1057	8.050
SD		0.35	68.19	15.04	29.33	117.9	53.28	0.300	145.4	2.210	241.4	0.120

Values less than LOD (limit of detection) were set to zero for statistical purposes

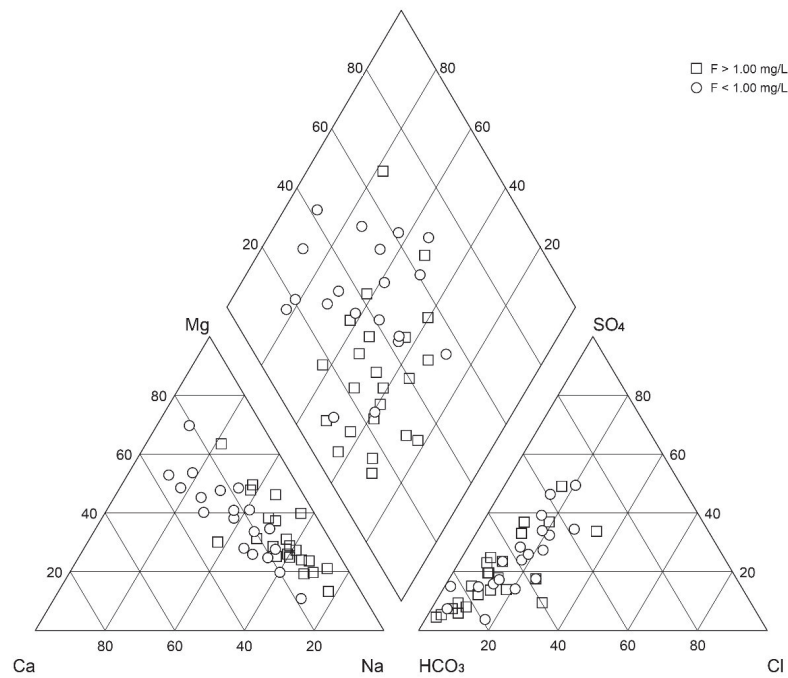


Fig. 2. Piper diagram representing groundwater facies of the study area.

standards (1.00 mg/L) for drinking water. The groundwater samples were divided into two groups based on China's drinking water guidelines (1.00 mg/L); the low-fluoride drinking groundwater group (<1.00 mg/L), and the high-fluoride drinking groundwater group (>1.00 mg/L).

#### High-Fluoride Geochemical Behaviours

In the high-fluoride drinking groundwater group, the pH was between 7.79 and 8.28, and the  $\text{Ca}^{2+}$  concentration ranged from 15.16 to 76.01 mg/L, with a mean of 34.26 mg/L. The  $\text{Na}^+$  concentration ranged from 86.53 to 311.24 mg/L, with a mean of 169.62 mg/L. The  $\text{HCO}_3^-$  concentration ranged from 321.58 to 853.02 mg/L, with a mean of 566.28 mg/L, whilst the TDS concentration ranged from 721 to 1564 mg/L, with a mean of 1057 mg/L (Table 1). In the low-fluoride drinking water group, the pH was between 7.20 and 8.06, and the  $\text{Ca}^{2+}$  concentration ranged from 35.53 to 69.20 mg/L, with a mean of 52.29 mg/L. The  $\text{Na}^+$  concentration ranged from 20.32 to 218.47 mg/L, with a mean of 106.84 mg/L. The  $\text{HCO}_3^-$  concentration ranged from 300.61 to 488.94 mg/L, with a mean of 421.75 mg/L, and the TDS concentration ranged from 319 to 1386 mg/L, with a mean of 838 mg/L.

The high-fluoride drinking water group had a higher  $\text{HCO}_3^-$  concentration and pH compared with low-fluoride drinking water. This suggests that an alkaline environment may promote the dissolution of  $\text{F}^-$  [15, 38]. The  $\text{F}^-$  concentration was found to clearly increase with decreasing  $\text{Ca}^{2+}$  content, showing a good negative correlation (Fig. 3b). The high-fluoride

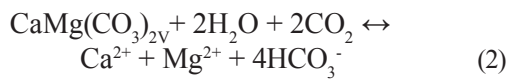
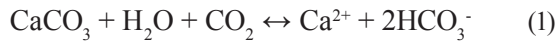
drinking water samples also had a slightly higher  $\text{Na}^+$  content and TDS, indicating that TDS and  $\text{Na}^+$  content are not dominant factors of the  $\text{F}^-$  content.

The majority of the groundwater samples with high  $\text{F}^-$  content were of the  $\text{Na}\cdot\text{Mg}\cdot\text{HCO}_3\cdot\text{SO}_4$  type (53.81%) and  $\text{Na}\cdot\text{Mg}\cdot\text{HCO}_3$  type (25.76%), as shown in Fig. 2. In comparison, most of the groundwater samples with low  $\text{F}^-$  content were of the  $\text{Na}\cdot\text{Mg}\cdot\text{HCO}_3$  type (85.71%). This indicates that the hydro-chemical facies of the high-fluoride drinking groundwater are more complex and diverse. Generally, the high-fluoride groundwater belonged to the  $\text{Na}\cdot\text{HCO}_3$  type, as dissolved  $\text{Na}^+$  and  $\text{Mg}^+$  promote elevated  $\text{F}^-$  concentrations in water [15, 16, 39, 40].

## Discussion

### Dissolution and Precipitation Process

Due to the poor solubility of  $\text{CaF}_2$ , if  $\text{CaF}_2$  gets dissolved in a water body, when the content of  $\text{Ca}^{2+}$  increases, the  $\text{F}^-$  content will decrease. The more rapid the rise in the  $\text{Ca}^{2+}$  content, the more accelerated the reduction in the  $\text{F}^-$  content. Fig. 3b) shows that the  $\text{Ca}^{2+}$  content in the high-fluoride groundwater samples was lower than that in the low-fluoride groundwater samples. Moreover, the high  $\text{HCO}_3^-$  content promotes the dissolution of  $\text{F}^-$ , as shown in Fig. 3d). The main source of  $\text{HCO}_3^-$  is the dissolution of calcite ( $\text{CaCO}_3$ ) and dolomite ( $\text{CaMg}(\text{CO}_3)_2$ ) [21]. Based on this evidence, the main factors that control the weathering process of  $\text{CaF}_2$  may be expressed as:



Based on Equations (1) and (2), the dissolution of  $\text{CaCO}_3$  and  $\text{CaMg}(\text{CO}_3)_2$  in the presence of  $\text{CO}_2$  generates a large amount of  $\text{Ca}^{2+}$ ,  $\text{Mg}^{2+}$ , and  $\text{HCO}_3^-$ .

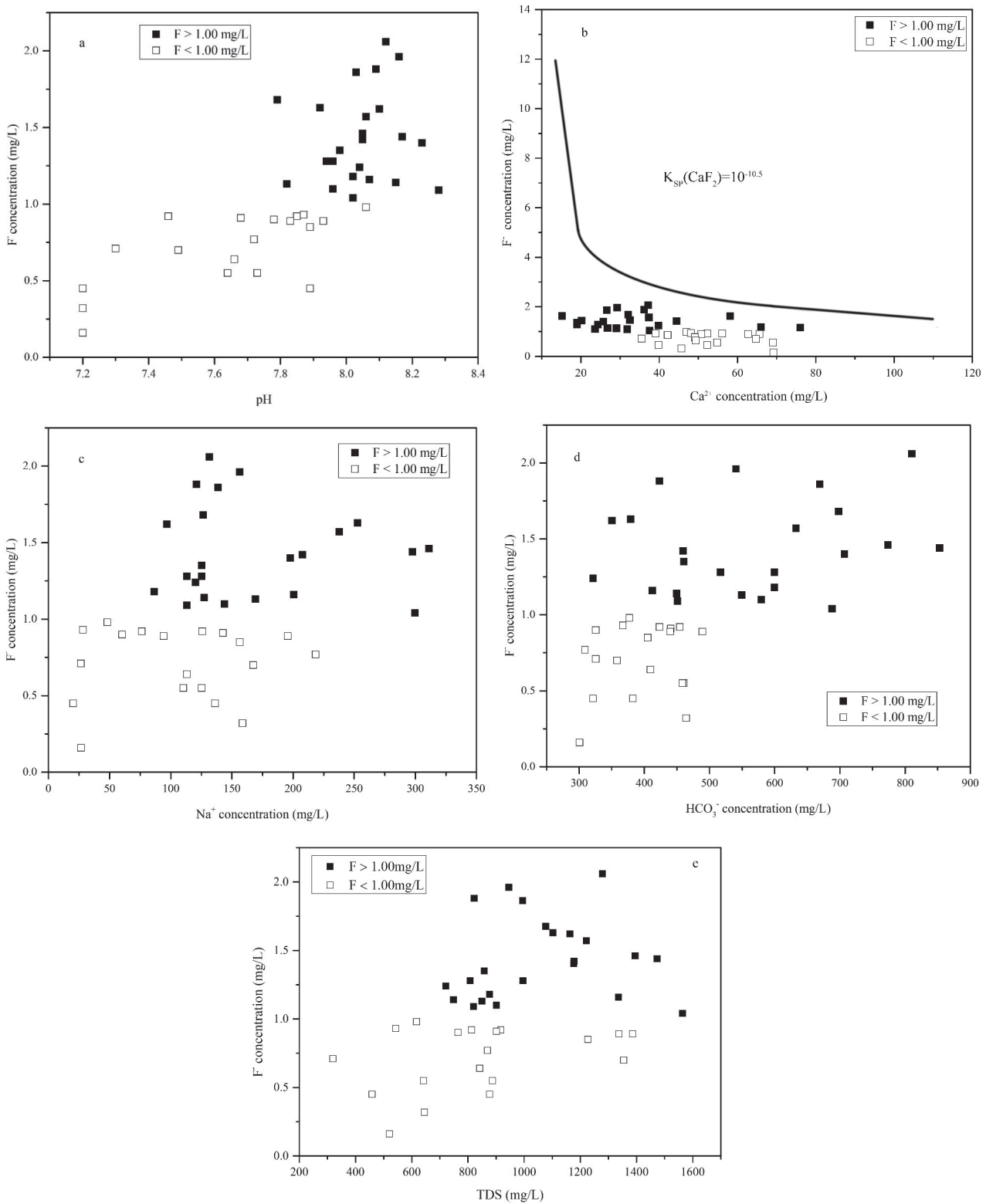


Fig. 3. Plots of a) pH versus  $\text{F}^-$ , b)  $\text{Ca}^{2+}$  versus  $\text{F}^-$ , c)  $\text{Na}^+$  versus  $\text{F}^-$ , d)  $\text{HCO}_3^-$  versus  $\text{F}^-$ , and e) TDS versus  $\text{F}^-$  of the drinking groundwater samples.

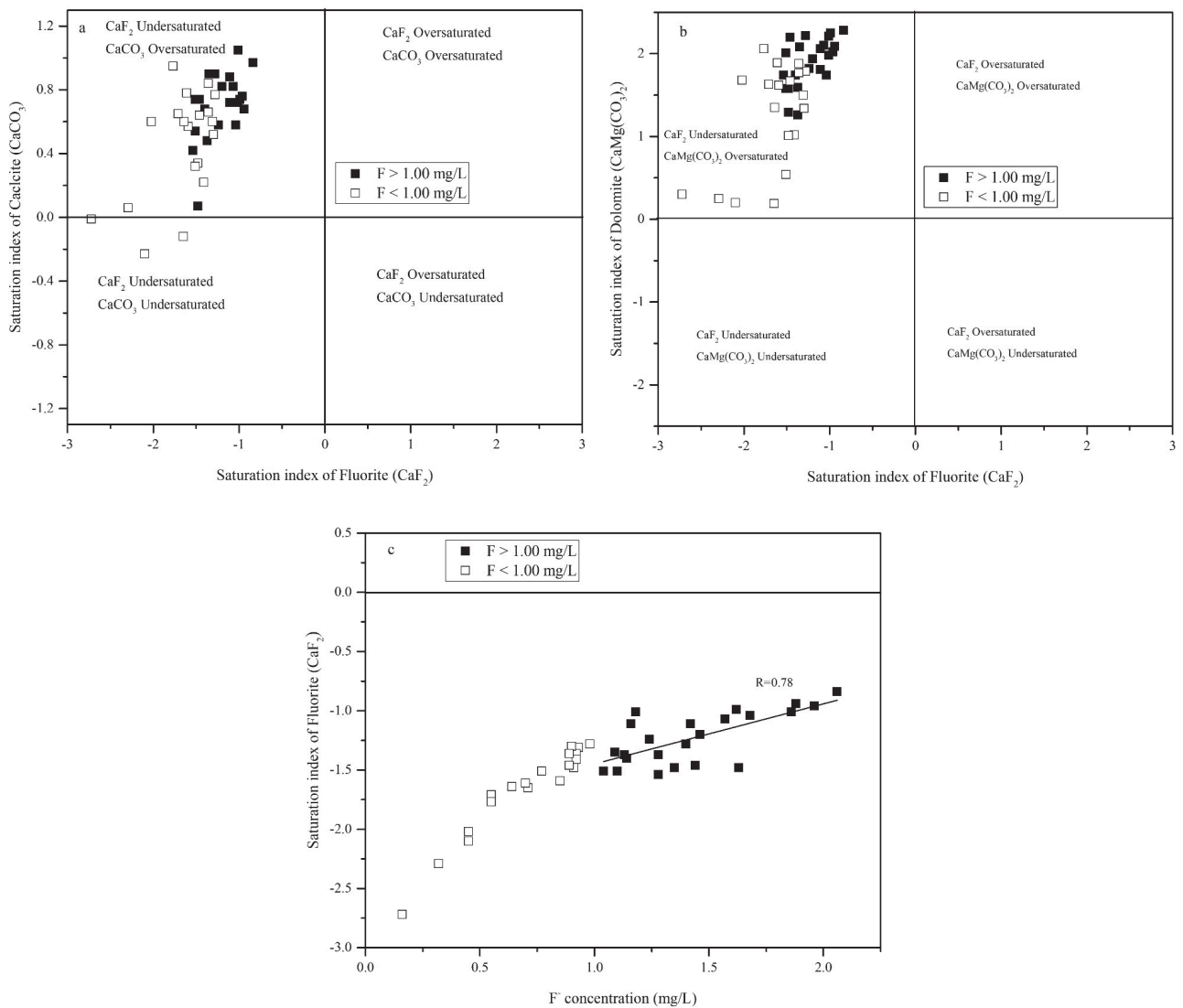


Fig. 4. Plots of a) the SI of calcite versus the SI of fluorite, b) the SI of dolomite versus the SI of fluorite, c) F versus the SI of fluorite.

The high HCO<sub>3</sub><sup>-</sup> concentration may cause a left shift in the equilibrium (i.e., Equation (3)), leading to an increase in F<sup>-</sup> content [41, 42].

The saturation index (SI) may be obtained from Equation (4) [40, 42]:

$$SI = \log_{10}(K_{IAP}/K_{sp}) \quad (4)$$

...where K<sub>IAP</sub> is the ion activity product of a particular solid phase and K<sub>sp</sub> is the solubility product of the phase. The SI is a reliable means to determine whether a groundwater body is oversaturated (SI>0), undersaturated (SI<0), or saturated (SI = 0) [43]. Fig. 4 plots the SIs of minerals in the groundwater samples, including calcite, dolomite, and fluorite.

All samples were undersaturated with respect to fluorite, indicating that the F<sup>-</sup> anions in the groundwater samples were mainly sourced from the dissolution of fluorite (CaF<sub>2</sub>) [18]. Fig. 4a) shows that the SI values of most high-fluoride groundwater samples were higher than those of the low-fluoride groundwater samples,

suggesting that the dissolution of fluorite (K<sub>sp</sub> = 10<sup>-10.5</sup>) has a higher influence on the high-fluoride groundwater group [38]. All high-fluoride groundwater samples were oversaturated with respect to dolomite and calcite. This is evidence demonstrating that the precipitation of dolomite and calcite reduces Ca<sup>2+</sup> content, promoting the dissolution of fluorite generating an elevated F<sup>-</sup> content [3, 40, 44].

Fig. 4c) shows the SI of fluorite (CaF<sub>2</sub>) versus the F<sup>-</sup> content (mg/L); this relationship may assist in determining the connection between fluorite dissolution and the F<sup>-</sup> content in the groundwater samples [43, 45]. The positive correlation (R = 0.78) between the F<sup>-</sup> concentration and the SI of fluorite (CaF<sub>2</sub>) in the high-fluoride drinking groundwater implies that fluorite dissolution plays a significant role in leaching F<sup>-</sup> into the groundwater [5, 43, 46].

The dissolution of other sources of fluoride, including biotite, phlogopite, and hornblende may also cause an increase in the Ca<sup>2+</sup> and Mg<sup>2+</sup> content [47, 48]. However, the high-fluoride groundwater samples

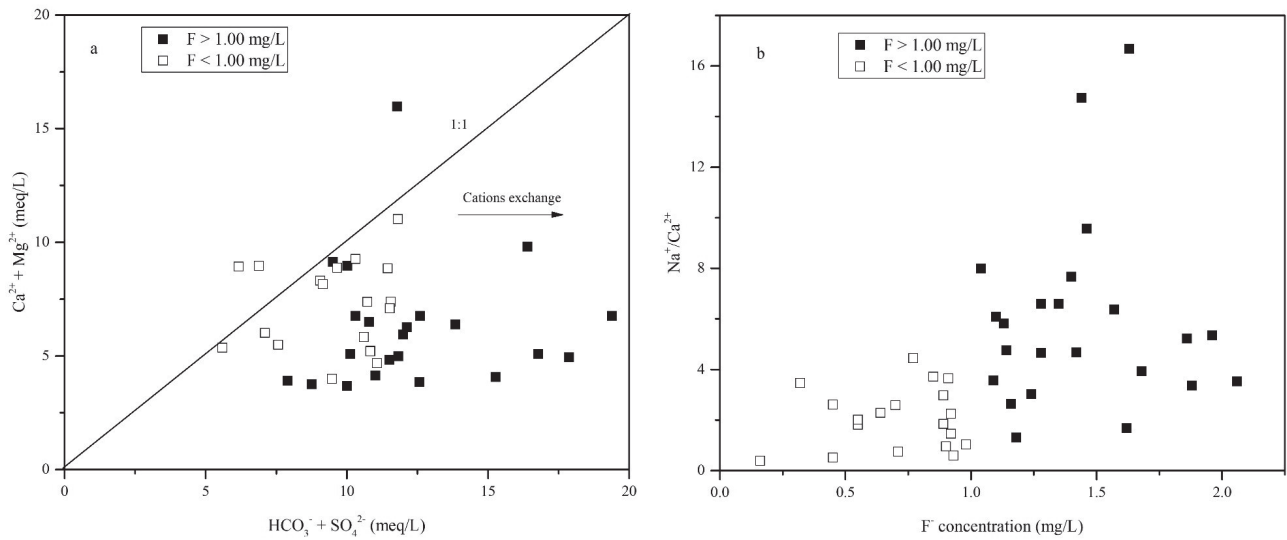


Fig. 5. Plots of a)  $(Ca^{2+}+Mg^{2+})$  versus  $(HCO_3^-+SO_4^{2-})$  and b)  $F^-$  versus  $Na^+/Ca^{2+}$  of the drinking groundwater samples.

collected in this study had low  $Ca^{2+}$  content. This may be attributable to the ion exchange interaction between the  $Ca^{2+}$  in groundwater and other cations (such as  $Na^+$ ) in clay minerals [49, 50].

The relationship between the  $Ca^{2+}+Mg^{2+}$  content and the  $HCO_3^-+SO_4^{2-}$  content is commonly used to analyse water-rock interactions in groundwater [49, 51]. Fig. 5a) shows that 92.86% of groundwater samples used for drinking water supply sit below the 1:1 dissolution line. This indicates that the dissolution of  $Ca^{2+}$  and  $Mg^{2+}$  into groundwater is more gradual than that of  $HCO_3^-$  and  $SO_4^{2-}$ . This evidence suggests that the dissolution of biotite, phlogopite, and hornblende plays a significant role in the groundwater geochemistry for the study area. Additionally, the high-fluoride groundwater samples contain more  $HCO_3^-$  and  $SO_4^{2-}$  (Fig. 5a) than the low-fluoride groundwater samples. Fig. 5b) shows the high  $Na^+/Ca^{2+}$  ratio ( $>1$ ), a favourable condition for fluoride

dissolution, which suggests that the  $Ca^{2+}$  in the high-fluoride groundwater has been exchanged by the  $Na^+$  in clay minerals, leading to a low  $Ca^{2+}$  content [52].

### Evaporation Factor

The Gibbs map was used to evaluate the contribution of the evaporation process, [5, 25, 53]. The TDS concentrations of the groundwater samples were plotted against the ratios of  $Na^+/(Na^++Ca^{2+})$  in Fig. 6a). It was found that 91.30% of the high-fluoride groundwater samples had  $Na^+/(Na^++Ca^{2+})$  values ranging between 0.80 and 1.00. These samples were in the evaporation crystallisation dominance field although outside the rock weathering field and the atmosphere precipitation dominance field (Fig. 6a). As such, evaporation is a dominant factor in geochemistry for increased  $F^-$  content in drinking water [22, 25, 41].

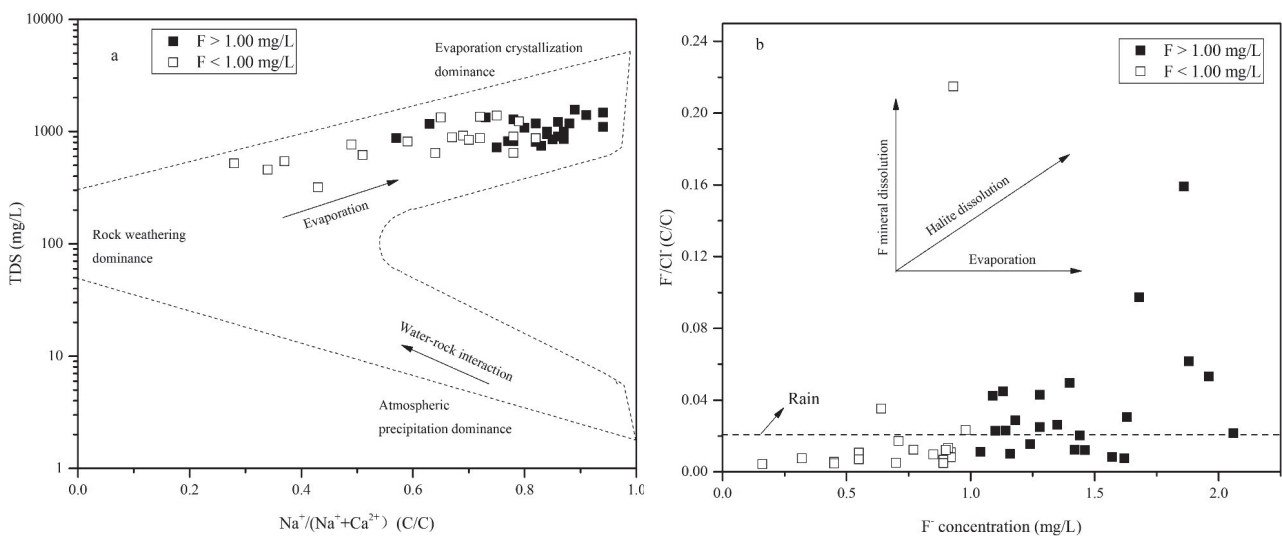


Fig. 6. Plots of a) Gibbs diagram and b)  $F^-$  versus  $F^-/Cl^-$  of the drinking groundwater samples.

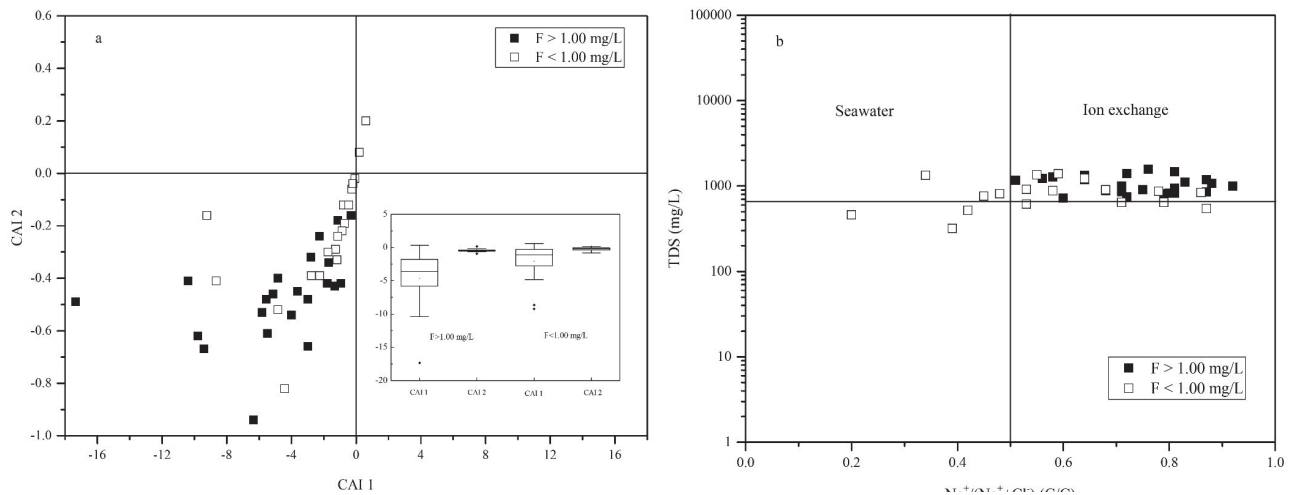


Fig. 7. Plots of a) CAI 1 versus CAI 2 and b) TDS versus Na<sup>+</sup>/(Na<sup>+</sup>+Cl<sup>-</sup>) of the drinking groundwater samples.

The F/Cl<sup>-</sup> ratio was plotted as a function of F<sup>-</sup> content in Fig. 6b), to investigate the influence of evaporation on the geochemical behaviour of fluoride in drinking water. When rainwater was the source of the F<sup>-</sup> cations, the groundwater samples were around the F/Cl<sup>-</sup> = 0.02 line [5, 16]. Moreover, a high F<sup>-</sup> content and a low F/Cl<sup>-</sup> value in a water body indicates that the main source of F<sup>-</sup> is F-bearing minerals formed during the evaporation process [4]. For 69.57% of the high-fluoride groundwater samples, the F/Cl<sup>-</sup> values exceeded 0.02 mg/L. This indicates that evaporation also contributes to elevated F<sup>-</sup> content in drinking water [16, 54]. Under the influence of evaporation, the concentrations of various ions in groundwater increase, and CO<sub>2</sub> escapes from the water body, resulting in an elevated TDS concentration (Table 1) and the precipitation of dolomite. This produces favourable conditions (low Ca<sup>2+</sup> and high Na<sup>+</sup> contents) for the dissolution of F<sup>-</sup> [10].

### Cation Exchange

Schoeller [55] proposed two indices (CAI 1 and CAI 2) to determine the possible ion-exchange reactions in groundwater. CAI 1 and CAI 2 may be calculated using Equations (5) and (6) (meq/L):

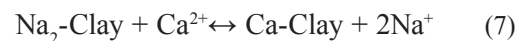
$$CAI\ 1 = [Cl^- - (Na^+ + K^+)] / Cl^- \quad (5)$$

$$CAI\ 2 = [Cl^- - (Na^+ + K^+)] / (SO_4^{2-} + HCO_3^- + CO_3^{2-} + NO_3^-) \quad (6)$$

If CAI 1 and CAI 2 are all positive, the K<sup>+</sup> and Na<sup>+</sup> in groundwater have been exchanged for Ca<sup>2+</sup> and Mg<sup>2+</sup>. In contrast, if CAI 1 and CAI 2 are negative, the Ca<sup>2+</sup> and Mg<sup>2+</sup> in groundwater have been exchanged by K<sup>+</sup> and Na<sup>+</sup>. Finally, if CAI 1 and CAI 2 are 0.00, the ion exchange reaction has not occurred in groundwater [49, 50, 56, 57]. Moreover, the larger the

CAI 1 and CAI 2 values, the stronger the ion exchange reaction.

Fig. 7a) shows that the CAI 1 and CAI 2 of high-fluoride groundwater samples were all negative, indicating that the Ca<sup>2+</sup> and Mg<sup>2+</sup> in groundwater were exchanged for K<sup>+</sup> and Na<sup>+</sup>. As a result, the Ca<sup>2+</sup> and Mg<sup>2+</sup> contents were lower than the K<sup>+</sup> and Na<sup>+</sup> content in drinking water, and the excess K<sup>+</sup> and Na<sup>+</sup> balance the HCO<sub>3</sub><sup>-</sup> and SO<sub>4</sub><sup>2-</sup> content (Fig. 5a). Fig. 8 shows the X-ray diffraction (XRD) spectrum of a sediment sample obtained from the study area, revealing its mineral composition. Clay minerals, such as montmorillonite and illite, were found throughout the study area, providing the environment for cation exchange [12]. The indices of high-fluoride groundwater samples scatter within a narrow range from -17.34 to -0.31, and from -0.94 to -0.18 for CAI 1 and CAI 2, respectively (Fig. 7a). The CAI 1 and CAI 2 values of the high-fluoride groundwater samples were much higher than the low-fluoride groundwater samples, suggesting that the ion exchange reaction is more intense in the former. As cation exchange contributes to the increase of Na<sup>+</sup> content in the high-fluoride groundwater, this high Na<sup>+</sup> content promotes the leaching of F<sup>-</sup> into the groundwater [8, 44]. The process may be described by Equation (7):



The relationship between TDS and Na<sup>+</sup>/(Na<sup>+</sup>+Cl<sup>-</sup>) is another significant piece of evidence demonstrating cation exchange in groundwater. If the Na<sup>+</sup> content in water is sourced from seawater, the Na<sup>+</sup>/(Na<sup>+</sup>+Cl<sup>-</sup>) value should theoretically be equal to or below 0.50, and the TDS value should be higher than 1000 mg/L. The Na<sup>+</sup>/(Na<sup>+</sup>+Cl<sup>-</sup>) of the collected samples was above 0.50, suggesting the occurrence of cation exchange during the formation of this groundwater resource (Fig. 7b). All samples were also within the ion exchange dominance field (Fig. 6a), indicating that excess Na<sup>+</sup> in the high-fluoride groundwater originates from cation exchange

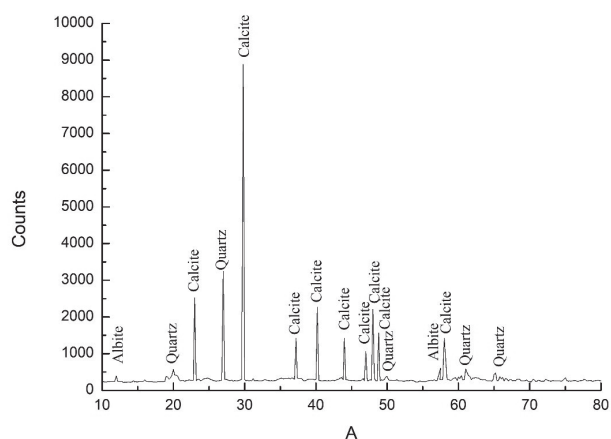


Fig. 8. XRD spectrum of a bulk sediment sample collected from the study area.

(Dehbandi et al. 2018). The dissolution of calcite and dolomite did not promote  $\text{Ca}^{2+}$  concentrations due to cation exchange (Equations (1) and (2)).

### Competitive Effect

In an alkaline environment,  $\text{OH}^-$  and  $\text{HCO}_3^-$  in groundwater competes with clay minerals for fluoride anions [60]. The  $\text{F}^-$  content in high-fluoride groundwater had a weak positive correlation with the  $\text{HCO}_3^-/(\text{HCO}_3^- + \text{Cl}^-)$  ratio, as shown in Fig. 9. This suggests that the adsorbed  $\text{F}^-$  on the surface of minerals may be released under high  $\text{HCO}_3^-$  conditions [10]. As such, the high  $\text{HCO}_3^-$  environment promotes the enrichment of  $\text{F}^-$  in groundwater by reducing the adsorption capability of minerals [5].

Fig. 3a) shows that the  $\text{F}^-$  concentration in the groundwater had a slight increasing trend in terms of its pH, which may be due to the competitive effect. In an alkaline environment, the surface of minerals is neutral or negatively charged, inhibiting the adsorption of  $\text{F}^-$  and leading to the release of  $\text{F}^-$  into the groundwater [10, 61].

### Anthropogenic Activities

$\text{NO}_3^-$  originates from untreated irrigation water, the infiltration of organic matter, synthetic fertilisers, and runoff from the surrounding agricultural fields [58, 59]; the  $\text{NO}_3^-$  content in the groundwater exceeds 5 mg/L [5, 59]. The relationship between the  $\text{F}^-$  and  $\text{NO}_3^-$  concentrations may aid in determining the influence of anthropogenic activities on groundwater.

The drinking water aquifer in this study area is a confined aquifer that exists within an anaerobic reduction environment. The  $\text{NO}_3^-$  content in the drinking water aquifer should be close to zero. However, 33.81% of the groundwater samples contained  $\text{NO}_3^-$ , whilst the  $\text{NO}_3^-$  content in 14.54% of the groundwater samples exceeded the pollution limit (5 mg/L). These

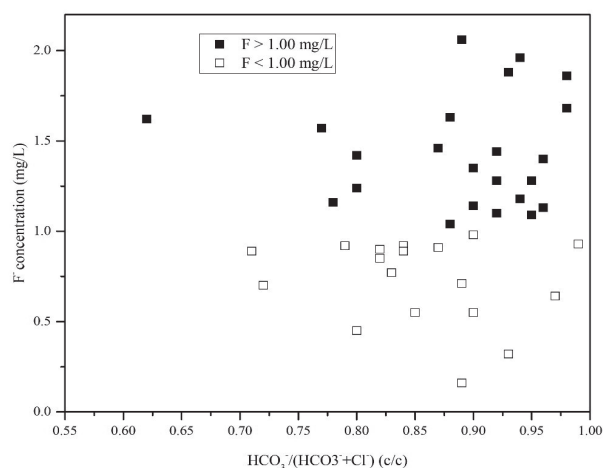


Fig. 9. Scatter plots of  $\text{HCO}_3^-/(\text{HCO}_3^- + \text{Cl}^-)$  versus the  $\text{F}^-$  content in drinking groundwater.

results suggest that part of the drinking water aquifer is significantly impacted by anthropogenic activities. The percentage of high-fluoride groundwater samples that contained  $\text{NO}_3^-$  was 33.33%; this is significantly higher than the low-fluoride groundwater samples (15.78%). The  $\text{NO}_3^-$  concentrations in two high-fluoride groundwater samples were 8.51 and 5.43 mg/L, respectively. The corresponding  $\text{F}^-$  concentrations in these two samples were 1.42 and 1.96 mg/L, respectively; this was higher than the mean  $\text{F}^-$  concentration (1.42 mg/L). The positive correlation between the  $\text{NO}_3^-$  and  $\text{F}^-$  content indicates that anthropogenic activities are important factors that contribute to the elevated  $\text{F}^-$  content in drinking water.

### Principal Component Analysis

To elucidate potential sources of variations in the hydrochemistry of the water resources in the study area, the pH and ion contents were statistically analysed using principal component analysis (PCA) [52, 62]. Three factors were extracted sequentially representing four different  $\text{F}^-$  sources, accounting for 80.99% of the total variables (cumulative) (Table 2).

The first factor (PC1) accounted for 34.47% of the total variables, which respectively, showed positive loadings with the  $\text{F}^-$  (0.56),  $\text{HCO}_3^-$  (0.62), and  $\text{Na}^+$  (0.40) content and a negative loading with the  $\text{Ca}^{2+}$  (-0.77) content, suggesting a potential natural source for the dissolution of F-bearing minerals in the study area [16, 52]. The second factor had a negative loading with the  $\text{Ca}^{2+}$  (-0.77) and  $\text{Na}^+$  (0.40) and  $\text{K}^+$  (0.34) content, indicating that cation exchange also governs the water chemistry [14]. The second component (PC2) accounted for 24.03% of the total variables, exhibiting a positive loading with the  $\text{Na}^+$ ,  $\text{K}^+$ ,  $\text{Ca}^{2+}$ ,  $\text{Mg}^{2+}$ ,  $\text{Cl}^-$ , TDS, and  $\text{SO}_4^{2-}$  content. However, all of these parameters were lower than 0.50, indicating a group effect. The positive loading of the cations ( $\text{Na}^+$ ,  $\text{Ca}^{2+}$ ,  $\text{Mg}^{2+}$ , and  $\text{K}^+$ ) explains their natural occurrence in water, potentially

Table 2. The PCA date for F- sources of the study area.

Variable	Component			
	1	2	3	4
pH	0.3942	-0.0742	0.2720	0.1114
Na <sup>+</sup>	0.4047	0.2436	-0.3459	0.0338
K <sup>+</sup>	-0.3368	0.0017	-0.3002	-0.1449
Ca <sup>2+</sup>	-0.7689	0.4217	-0.0529	0.4245
Mg <sup>2+</sup>	-0.0126	0.3826	0.4312	-0.5276
Cl <sup>-</sup>	0.1819	0.4828	0.0090	-0.0666
SO <sub>4</sub> <sup>2-</sup>	0.2156	0.4843	-0.0191	0.2145
HCO <sub>3</sub> <sup>-</sup>	0.6237	-0.2461	-0.4331	-0.1120
F <sup>-</sup>	0.5619	-0.2097	0.3255	-0.3185
NO <sub>3</sub> <sup>-</sup>	0.1215	-0.2382	0.4306	0.6849
TDS	0.4538	0.4019	-0.2197	0.0186
% of variance	34.47	24.03	11.81	10.68
Cumulative %	34.47	58.50	70.31	80.99

due to weathering and the dissolution of minerals. The increased contribution of anions (SO<sub>4</sub><sup>2-</sup> and Cl<sup>-</sup>) and decreased contribution of HCO<sub>3</sub><sup>-</sup> (-0.25) was also evidenced in the TDS, which may be attributed to the evaporation effect [52, 62, 63]. The third component accounts for 11.81% of the total variables showing positive loadings with the F<sup>-</sup> (0.33) and Mg<sup>2+</sup> (0.42) and NO<sub>3</sub><sup>-</sup> (0.43) content and pH (0.27), and negative loadings with the HCO<sub>3</sub><sup>-</sup> (-0.43) content; this may be a possible source for the competitive effect. The final component

(PC4), was the lowest and accounted for 10.68% of the total variables. It showed only a strong correlation (0.68) with the NO<sub>3</sub><sup>-</sup> content, which was sourced from anthropogenic activities.

Fluoride Formation Mechanisms Discussion

Fig. 10 provides a schematic that elucidates the fluoride enrichment process for the groundwater in the study area.

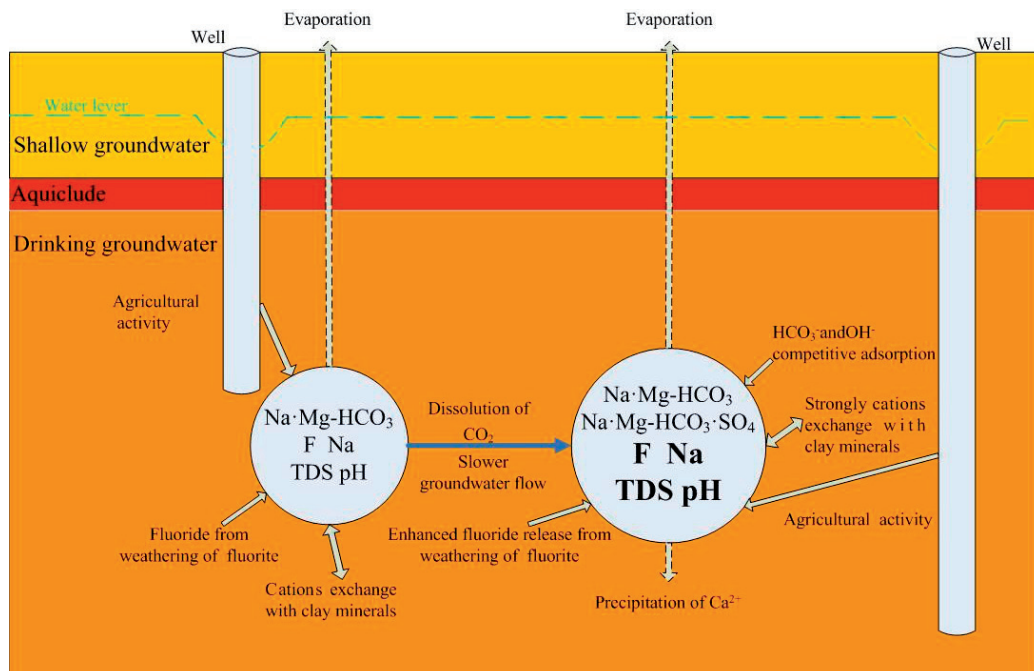


Fig. 10. Mechanism of the formation of the high-fluoride drinking groundwater (left to right).

It is proposed that the initial F<sup>-</sup> in groundwater is mainly sourced from the weathering of F-bearing minerals, cation exchange, the competitive effect, and agricultural activities. The initial hydro-chemical facies of the groundwater was the Na-Mg-HCO<sub>3</sub> type. With the gradual reduction in groundwater flow, an increasing amount of CO<sub>2</sub> dissolves, causing a rise in the pH of groundwater, whilst the TDS of groundwater gradually increases. With Ca<sup>2+</sup> precipitation, the TDS and Na<sup>+</sup> content in groundwater had become the dominant factors, and the diversity of hydro-chemical facies of the groundwater had increased (Na-Mg-HCO<sub>3</sub> type and Na-Mg-HCO<sub>3</sub>·SO<sub>4</sub><sup>2-</sup> type).

The increases in pH, HCO<sub>3</sub><sup>-</sup>, and TDS provided suitable conditions to form high-fluoride content water. The weathering of F-bearing minerals and cation exchange with clay minerals promoted the dissolution of F<sup>-</sup> into the groundwater system. Additionally, agricultural activities and competitive effects were important factors that contributed to the elevated F<sup>-</sup> content. All of these factors contributed to fluoride enrichment in the groundwater beyond the permissible limits as per China's drinking water regulations, generating a drinking water supply that is considered to have a high content of fluoride.

### Conclusions

Few studies exist on the spatial distribution and geochemical behaviour of F<sup>-</sup> in drinking water aquifers in coal-mining areas. As such, the sources and mechanism behind high-fluoride groundwater have not yet been fully understood. The present study attempts to understand the spatial distribution of F<sup>-</sup> in groundwater used as a drinking water source in the Sulin coal-mining district. It also identifies major geochemical processes and formation mechanisms controlling the fluoride content in this groundwater resource. The findings of this study include:

(1) The F<sup>-</sup> concentrations in the groundwater samples were between 0.16 and 2.06 mg/L, with a mean of 1.11 mg/L. In addition, 54.76% of the groundwater samples exceeded China's national standards (1.00 mg/L);

(2) The high-fluoride groundwater (>1.00 mg/L) had a higher pH and HCO<sub>3</sub><sup>-</sup> content compared to the low-fluoride groundwater (<1.00 mg/L). The hydro-chemical facies reflect that low-fluoride groundwater was confined to the Na-Mg-HCO<sub>3</sub> type. Hydrogeochemical investigations revealed that the fluoride content was associated with the Na-Mg-HCO<sub>3</sub>·SO<sub>4</sub> and Na-Mg-HCO<sub>3</sub> types;

(3) Several geochemical processes, such as evaporation, F-bearing mineral dissolution, cation exchange, competitive effects, and anthropogenic activities, were identified as the primary mechanisms for F<sup>-</sup> enrichment in the groundwater. PCA also demonstrated that F<sup>-</sup> also increased the contribution

of the HCO<sub>3</sub><sup>-</sup> and Na<sup>+</sup> content and decreased the contribution of Ca<sup>2+</sup> in PC1 (34.47%). This indicates that F-bearing minerals were the main source of F<sup>-</sup> in the groundwater. Positive loadings of Na<sup>+</sup>, K<sup>+</sup>, Ca<sup>2+</sup>, Mg<sup>2+</sup>, Cl<sup>-</sup>, TDS, and SO<sub>4</sub><sup>2-</sup> in PC2 (24.03%), suggested an evaporation effect. The positive loadings with F<sup>-</sup>, pH, NO<sub>3</sub><sup>-</sup>, and negative loadings with HCO<sub>3</sub><sup>-</sup> in PC3 (11.81%), indicate the potential for the competitive effect. The final PC4 (10.68%) showed a strong correlation with the NO<sub>3</sub><sup>-</sup> content, highlighting sources from human activity.

This research will aid in improving the cognition of fluoride geochemical behaviours in coal-mining districts and assist the informed management of groundwater resources for drinking in efforts to improve public safety within the study area.

### Acknowledgements

Funding: This work was supported by the Open Fund of State Key Laboratory of Groundwater Protection and Utilization by Coal Mining (grant number SHJT-17-42.17), the Ecological restoration project in Lengshuijiang Antimony Mine area (grant number LCG2020009), and the Fundamental Research Funds for the Central Universities of China (grant number 3142018009). We would like to thank Editage (www.editage.cn) for English language editing.

### Conflict of Interest

The authors declare no conflict of interest.

### References

- XIAO J., JIN Z., ZHANG F. Geochemical controls on fluoride concentrations in natural waters from the middle Loess Plateau, China. *J Geochem Explor*, **159**, 252, **2015**.
- ALI S., SHEKHAR S., BHATTACHARYA P., VERMA G., CHANDRASEKHAR T., CHANDRASHEKHAR A.K. Elevated fluoride in groundwater of Siwani Block, Western Haryana, India: A potential concern for sustainable water supplies for drinking and irrigation. *Groundwater for Sustainable Development*, **7**, 410, **2018**.
- RASHID A., GUAN D.X., FAROOQI A., KHAN S. Fluoride prevalence in groundwater around a fluorite mining area in the flood plain of the River Swat, Pakistan. *Sci Total Environ*, **635**, 203, **2018**.
- OLAKA L.A., WILKE F.D.H., OLAGO D.O., ODADA E.O., MULCH A., MUSOLFF A. Groundwater fluoride enrichment in an active rift setting: Central Kenya Rift case study. *Sci Total Environ*, **545-546**, 641, **2016**.
- LI D., GAO X., WANG Y., LUO W. Diverse mechanisms drive fluoride enrichment in groundwater in two neighboring sites in northern China. *Environ Pollut*, **237**, 430, **2018**.
- MONDAL D., GUPTA S., REDDY D.V., NAGABHUSHANAM P. Geochemical controls on fluoride concentrations in groundwater from alluvial aquifers of the

- Birbhum district, West Bengal, India. *J Geochem Explor*, **145**, 190, **2014**.
7. WHO World Health Organization. Health criteria and other supporting information, **2<sup>nd</sup> ed. Geneva, Switzerland: WHO**, 940, **1984**.
  8. DEHBANDI R., MOORE F., KESHAVARZI B. Geochemical sources, hydrogeochemical behavior, and health risk assessment of fluoride in an endemic fluorosis area, central Iran. *Chemosphere*, **193**, 763, **2018**.
  9. RAFIQUE T., NASEEM S., USMANI T.H. Geochemical factors controlling the occurrence of high fluoride groundwater in the Nagar Parkar area, Sindh. Pak. *J. Hazard Mater* **171**, 424, **2009**.
  10. ABU RUKAH Y., ALSOKHNY K. Geochemical assessment of groundwater contamination with special emphasis on fluoride concentration, North Jordan. *Geochemistry*, **64** (2), 171, **2004**.
  11. MAO R., GUO H., JIA Y. Distribution characteristics and genesis of fluorine groundwater in the Hetao basin, Inner Mongoli. *Earth Science Frontiers*, **23** (2), 260, **2016**.
  12. LI C., GAO X., WANG Y. Hydrogeochemistry of high-fluoride groundwater at Yuncheng Basin, northern China. *Sci Total Environ*, **508**, 155, **2015**.
  13. YANG N., LIU J., LIAO A. Distribution and formation factors of high fluoride deep groundwater in typical area of north Anhui Province. *HYDROGEOLOGY & ENGINEERING GEOLOGY*, **44**, 33, **2017**.
  14. WU C. Hydrogeochemistry and groundwater quality assessment of high fluoride levels in the Yanchi endorheic region, northwest China. *Appl Geochem*, **98**, 404, **2018**.
  15. HE J., AN Y., ZHANG F. Geochemical characteristics and fluoride distribution in the groundwater of the Zhangye Basin in Northwestern China. *J Geochem Explor*, **135**, 22, **2013**.
  16. SAJIL KUMAR P.J., JEGATHAMBAL P., NAIR S., JAMES E.J. Temperature and pH dependent geochemical modeling of fluoride mobilization in the groundwater of a crystalline aquifer in southern India. *J Geochem Explor*, **156**, 1, **2015**.
  17. GOMEZ M.L., BLARASIN M.T., MARTÍNEZ D.E. Arsenic and fluoride in a loess aquifer in the central area of Argentina. *Environ Geol*, **57** (1), 143, **2008**.
  18. THAPA R., GUPTA S., GUPTA A., REDDY D.V., KAUR H. Geochemical and geostatistical appraisal of fluoride contamination: An insight into the Quaternary aquifer. *Sci Total Environ*, **640-641**, 406, **2018**.
  19. BIDDAU R., CIDU R., LORRAI R., MULAS M.G. Assessing background values of chloride, sulfate and fluoride in groundwater: A geochemical-statistical approach at a regional scale. *J Geochem Explor*, **181**, 243, **2017**.
  20. DENG Y., NORDSTROM D.K., MCCLESKEY R.B. Fluoride geochemistry of thermal waters in Yellowstone National Park: I. Aqueous fluoride speciation. *Geochim Cosmochim Acta*, **75** (16), 4476, **2011**.
  21. JACKS G., BHATTACHARYA P., CHAUDHARY V., SINGH K.P. Controls on the genesis of some high-fluoride groundwaters in India. *Appl Geochem*, **20** (2), 221, **2005**.
  22. RAFIQUE T., NASEEM S., OZSVATH D., HUSSAIN R., BHANGER M.L., USMANI T.H. Geochemical controls of high fluoride groundwater in Umarkot Sub-District, Thar Desert, Pakistan. *Sci Total Environ*, **530-531**, 271, **2015**.
  23. RAJ D., SHAJI E. Fluoride contamination in groundwater resources of Alleppey, southern India. *Geosci Front*, **8** (1), 117, **2017**.
  24. PANASKAR D.B., WAGH V.M., MULEY A.A. Evaluating groundwater suitability for the domestic, irrigation, and industrial purposes in Nanded Tehsil, Maharashtra, India, using GIS and statistics. *Arab J Geosci*, **9**, 615, **2016**.
  25. LAXMANKUMAR D., SATYANARAYANA E., DHAKATE R. Hydrogeochemical characteristics with respect to fluoride contamination in groundwater of Maheshwarm mandal, RR district, Telangana state, India. *Groundwater for Sustainable Development*, **8**, 474, **2019**.
  26. CHEN L., XIE W.P., FENG X.Q., ZHANG N.Q. Formation of hydrochemical composition and spatio-temporal evolution mechanism under mining-induced disturbance in the Linhuan coal-mining district. *Arab J Geosci*, **10** (3), **2017**.
  27. DIANSH D., LIU G.J., FU B. Characteristics of the coal quality and elemental geochemistry in Permian coals from the Xinjier mine in the Huainan Coalfield, north China: Influence of terrigenous inputs. *J Geochem Explor*, **186**, 50, **2018**.
  28. SUN L., GUI H., CHEN S. Geochemistry of sandstones from the Neoproterozoic Shijia Formation, northern Anhui Province, China: Implications for provenance, weathering and tectonic setting. *Geochemistry*, **72** (3), 253, **2012**.
  29. SUN L., GUI H., SONG C. Use of Geochemical Inversion to Study Deep Groundwater Runoff Pattern in Northern Anhui Mining Areas. *Coal Geology of China*, **21** (1), 35, **2009**.
  30. GUI H., L. CHEN L.W. Study on hydrogeological feature of the main pouring water aquifers within the mining area in northern Anhui. *Journal of China Coal Society*, **29** (3), 323, **2004**.
  31. LIN M., GUI H., PENG W. Health Risk Assessment of Heavy Metals in Deep Groundwater from Different Aquifers of a Typical Coal Mining Area: A Case Study of a Coal Mining Area in Northern Anhui Province. *ACTA GEOSCIENTICA SINICA* **35** (5), 589, **2014**.
  32. DAI X., LIU X., LI L. Discussion and countermeasures on safe drinking water in the rural areas of China. *Acta Geographica Sinica*, **62**, 907, **2007**.
  33. QIU H., GUI H. Heavy metals contamination in shallow groundwater of a coal-mining district and a probabilistic assessment of its human health risk. *Human and Ecological Risk Assessment: An International Journal*, **25** (3), 548, **2019**.
  34. WANG M. Hydrogeochemical Characteristics and Water Quality Evaluation of Carboniferous Taiyuan Formation Limestone Water in Sulin Mining Area in Northern Anhui, China. *Int J Environ Res Public Health*, **16** (14), **2019**.
  35. QIU H. Hydrogeochemical characteristics and water quality assessment of shallow groundwater: a case study from Linhuan coal-mining district in northern Anhui Province, China. *Water Supply*, **19** (5), 1572, **2019**.
  36. MHPRC. Standards for Drinking Water Quality. GB, **5749**, **2006**.
  37. PIPER M. Graphic procedure in the geochemical interpretation of water-analyses. *Hydrology*, 914, **1944**.
  38. BRINDHA K., JAGADESHAN G., KALPANA L., ELANGO L. Fluoride in weathered rock aquifers of southern India: Managed Aquifer Recharge for mitigation. *Environ Sci Pollut Res*. **2016**.
  39. AMINI M. Statistical modeling of global geogenic fluoride contamination in groundwaters. *Environ. Sci. Technol*, **42**, 3662, **2008**.
  40. KUMAR P., SINGH C.K., SARASWAT C., MISHRA B., SHARMA T. Evaluation of aqueous geochemistry of

- fluoride enriched groundwater: A case study of the Patan district, Gujarat, Western India. *Water Sci*, **31** (2), 215, **2019**.
41. HE X., MA T., WANG Y.X., SHAN H.M., DENG Y.M. Hydrogeochemistry of high fluoride groundwater in shallow aquifers, Hangjinhouqi, Hetao Plain. *J GEOCHEM EXPLOR*.135 63, **2013**.
  42. GARRELS R.M., MACKENZIE F.T. Evolution of Sedimentary Rocks. Norton and Company. New York, pp: 394, **1971**.
  43. ALI W., ASLAM M.W., JUNAID M., ALI K., GUO Y., RASOOL A., ZHANG H. Elucidating various geochemical mechanisms drive fluoride contamination in unconfined aquifers along the major rivers in Sindh and Punjab, Pakistan. *Environ Pollut*, **249**, 535, **2019**.
  44. ENALOU H.B., MOORE F., KESHAVARZI B. Source apportionment and health risk assessment of fluoride in water resources, south of Fars province, Iran\_ Stable isotopes ( $\delta^{18}\text{O}$  and  $\delta\text{D}$ ) and geochemical modeling approaches *Appl Geochem* **98**, 197, **2018**.
  45. PETTENATI M., PERRIN J., PAUWELS H. Simulating fluoride evolution in groundwater using a reactive multicomponent transient transport model: application to a crystalline aquifer of Southern India. *Appl. Geochem*, **29**, 102, **2013**.
  46. BRAHMAN K.D., KAZI T.G., AFRIDI N.H.I. Evaluation of high levels of fluoride, arsenic species and other physicochemical parameters in underground water of two sub districts of Tharparkar, Pakistan: a multivariate study. *Water Res*, **47**, 1005, **2013**.
  47. BRINDHA K., ELANGO L. Geochemistry of Fluoride Rich Groundwater in a Weathered Granitic Rock Region, Southern India. *Water Qual Expos Hea*, **5** (3), 127, **2013**.
  48. KALPANA L., BRINDHA K., ELANGO L. FIMAR: A new Fluoride Index to mitigate geogenic contamination by Managed Aquifer Recharge. *Chemosphere*, **220**, 381, **2019**.
  49. ZHU G.F., SU Y.H., HUANG C.L., FENG Q., LIU Z.G. Hydrogeochemical processes in the groundwater environment of Heihe River Basin, northwest China. *Environ Earth Sci*, **60** (1), 139, **2009**.
  50. WANG H.,JIANG X.W.,WAN L.,HAN G.L., GUO H.Hydrogeochemical characterization of groundwater flow systems in the discharge area of a river basin. *J Hydrol*, **527**, 433, **2015**.
  51. JALALI M. Major ion chemistry of groundwaters in the Bahar area, Hamadan, western Iran. *Environ Geol*, **47** (6), 763, **2005**.
  52. KUMAR S., VENKATESH A.S., SINGH R., UDAYABHANU G., SAHA D. Geochemical signatures and isotopic systematics constraining dynamics of fluoride contamination in groundwater across Jamui district, Indo-Gangetic alluvial plains, India. *Chemosphere*, **205**, 493, **2018**.
  53. GIBBS R. Mechanisms controlling world's water chemistry. *Science* **170**, 1088, **1970**.
  54. CURRELL M., CARTWRIGHT I., RAVEGGI M. Controls on elevated fluoride and arsenic concentrations in groundwater from the Yuncheng Basin, China. *Appl. Geochem*, **26** (4), 540, **2011**.
  55. SCHOELLER. Hydrodynamique dans le karst [Hydrodynamics of karst]. Actes du Colloques de Doubronik, IAHS/UNESCO,Wallingford, UK and Paris, France, 3, **1965**.
  56. KIM K.,RAJMOHAN, N.,KIM H.J.,HWANG G.S.,CHO M.J. Assessment of groundwater chemistry in a coastal region (Kunsan, Korea) having complex contaminant sources: a stoichiometric approach. *Environ Geol*, **46** (6-7), 763, **2004**.
  57. KAUR L., RISHI M.S. Hydrogeochemical characterization of groundwater in alluvial plains of river Yamuna in northern India: An insight of controlling processes. *J King Saud Univ Sci*, **2019**.
  58. SHARMA S.K., SUBRAMANIAN V. Hydrochemistry of the Narmada and Tapti Rivers, India. *Hydrol Process*, **22** (17), 3444, **2008**.
  59. HEATON T.H.E. Isotopic studies of nitrogen pollution in the hydrosphere and atmosphere: a review. *Chem. Geol. Isot. Geosci. Sect*, **59**, 87, **1986**.
  60. SU C., PULS R. Arsenate and arsenite removal by zerovalent iron : Effects of Phosphate, Silicate, Carbonate, Borate, Sulfate, Chromate, Molybdate and nitrate relative to Chloride. *Environ Sci Technol* **35** (22), 4562, **2001**.
  61. GUO H., ZHANG Y., XING L., JIA Y.F. Spatial variation in arsenic and fluoride concentrations of shallow groundwater from the town of Shapai in the Hetao basin, Inner Mongolia. *Appl Geochem* **27** (11), 2187, **2012**.
  62. EMENIKE C.P., TENEBE I.T., JARVIS P. Fluoride contamination in groundwater sources in Southwestern Nigeria: Assessment using multivariate statistical approach and human health risk. *Ecotoxicol Environ Saf*, **156**, 391, **2018**.
  63. KESHAVARZI B., MOORE F., ESMAEILI A., RASTMANESH F. The source of fluoride toxicity in Muteh area, Isfahan, Iran. *Environ Earth Sci*, **61** (4), 777, **2010**.